This is the final author version: The article is published as "Low temperature Fluorescence Study of Crude Petroleum Oils". P. Owens and A.G. Ryder, Energy & Fuels, in press, (2011). DOI: 10.1021/ef201030t

Low temperature fluorescence studies of crude petroleum oils.

Peter Owens and Alan G. Ryder.*

Nanoscale Biophotonics Laboratory, School of Chemistry,

National University of Ireland Galway, Galway, Ireland.

* Corresponding author.

Dr. Alan G. Ryder, Nanoscale Biophotonics Laboratory, School of Chemistry, National University of Ireland – Galway, Galway, Ireland.

Email: alan.ryder@nuigalway.ie

Abstract:

We have studied the low-temperature (133−298 K) fluorescence emission of crude petroleum oils using a combination of steady-state and time-resolved measurements. This was done to first see if we could generate linear correlations between oil composition information and the fluorescence measurements, and second to better understand how static and dynamic quenching affect fluorescence emission. It was observed that the fluorescence intensity and lifetime of the crude oils increased rapidly with decreasing temperature down to the freezing point and then either remained constant *or* surprisingly began to decrease slightly. These changes could not be correlated accurately with the compositional data available. However, despite the very large variations in sample composition, it was found that these lifetime-temperature changes followed simple Arrhenius and Eyring behavior. For the cold liquid phase, an Arrhenius model enabled the calculation of an intrinsic lifetime, the magnitude of which was inversely related to the degree of static quenching. The low values of the calculated activation energies (4.6 to 19.2 $kJmol^{-1}$) implied that in the liquid phase, non-radiative decay was primarily diffusion based quenching. At the lowest temperatures, when all samples have solidified, the lifetime data followed Eyring like behavior, giving typical enthalpy and entropy values of -1 $kJmol^{-1}$ and from -67 to -93 $JK^{-1}mol^{-1}$ respectively. The Eyring model was used to describe the non-radiative decay mechanism arising from vibrational coupling from the fluorophores to the surrounding matrix. This modeling of the temperature dependence of fluorescence lifetime has provided a clearer, quantitative picture of the fluorescence quenching processes in crude petroleum oils.

Key words: Fluorescence Lifetime, Crude Oil, Petroleum, Quenching, Energy transfer.

Introduction

The intrinsic fluorescence emission of crude petroleum oils has been noted since the 1870's,[1] and has been studied in detail at ambient temperatures by many different research groups.[2] In general, heavy oils have weak, broad, redder, and short-lived fluorescence emission while the lighter oils have stronger, narrower, bluer, and longer lived emission.[3-5] The character of fluorescence emission from petroleum oils is largely governed by Energy Transfer (ET) and quenching effects, which are very significant because of the relatively high concentrations of fluorophores and quenchers present in crude oils.[2,3,6] Petroleum and crude oils have been shown to follow systematic quenching behavior and Stern-Volmer analysis shows that a simple collisional model can be used to explain quenching in dilute solutions of crude oils.[4,7,8]

The effect of elevated temperature on crude oil fluorescence (using a sample set of eight oils) was studied in detail and it was found that fluorescence intensity decreased with increasing temperatures over 300 K.[9] The intensity changes were modeled using a simple Arrhenius model which gave indicative activation energies for thermal quenching of between 10 and 20 $kJmol^{-1}$. The authors also postulated that since the spectral profile of the oils seemed to be relatively independent of temperature, the individual fluorophore populations that are present in the oils have similar thermal quenching characteristics. The effect of high temperature on the fluorescence emission of other complex hydrocarbon based/derived materials such as kerogens, crude oils or coal has also been studied by a variety of research groups.[10-13]

Fluorescence emission is generally enhanced by lowering the temperature due to a reduction in collisional quenching.[14] For simple Polycyclic Aromatic Hydrocarbons (PAHs) systems (i.e. the sample contains no more than 4-5 different fluorophores), one can use low temperature studies to

investigate vibronic structure. One technique that can be applied is the Shpol'skii method which involves dissolving the PAHs in n-alkane solvents and then rapidly freezing to 77K or lower.[15,16] The method has been applied to the analysis of fluorophores in simple systems, such as the analysis of HPLC fractions (where sample complexity has been reduced by chromatographic means) which compared favorably with GC-Mass spectrometry for the resolution of five ring PAH isomers such as methylphenanthrene.[17] A similar approach has been used to determine methylbenzo[a]pyrene isomers in coal tar extracts.[18] Coupling the Schpol'skii method with synchronous fluorescence measurements has been applied to the quantitative analysis of various PAH's in mixtures and airborne particulates.[19] Shpol'skii methods have been combined with time resolved methods to achieve even higher selectivity in simple PAH mixture analysis.[20,21] More recently, the resolution of spectra from PAH mixtures was enhanced by lowering the temperature to that of liquid helium (4.2 K) and coupling the spectral data with fluorescence lifetime data in the form of a wavelength-decay time matrix.[22] As the sample complexity increases, the Schpol'skii method becomes less useful because the fluorophore identity and concentration is often unknown. For petroleum based fluids like crude oils, one has to extensively dilute the sample to ppm concentration levels, to generate better spectral structure in the emission. Following this procedure, one can discriminate highly diluted fuel oils at low temperature because of the structured nature of the emission.[23] This fact was later exploited for the forensic analysis of petroleum oil types.[24, 25] Measurement at low (77 K) temperatures also permits the collection of phosphorescence spectra from diluted crude oils.[26] However, it has to be noted that dilution of crude petroleum oils radically changes the photophysics of fluorescence emission and as such the Shpol'skii method is not suitable for exploring crude oil fluorescence

from neat, undiluted oils. We also note here, that there seems to be no published studies on the low temperature fluorescence emission of crude petroleum oils.

Previous studies of crude oils at room temperature have shown that fluorescence lifetimes are largely governed by a combination of dynamic and static effects, and that it was not possible to obtain accurate correlations between chemical composition data and lifetime measurements.[27-31] Here we have undertaken a detailed series of low-temperature time-resolved fluorescence measurements on crude petroleum oils to firstly observe the differences in fluorescence emission caused by lowering the temperature. Secondly to see if it is possible to obtain better quantitative correlations between chemical compositional data, and thirdly to quantify the effect of the various non-radiative processes on crude petroleum oil fluorescence emission.

Experimental Section

Samples and temperature control. The 20 oil samples were sourced from diverse geographical locations and rock types and the physical and chemical properties have been previously published in detail.[29,30] Methyl-cyclohexane (MeCH) and Methyl-cyclopentane (MeCP) were obtained from Sigma-Aldrich and used without further purification. A 3:2 (v/v) solvent mixture of MeCH and MeCP was used to dilute the oils since this solvent mixture forms a clear glass at liquid nitrogen temperatures.[32] An aliquot of petroleum oil was weighed out that was equivalent to 1 ml (calculated using oil density values). This was diluted with the appropriate amount of the solvent mixture to make a 1:5 stock solution and subsequent dilutions were serially diluted from this. This weighing method was used because it is impossible to accurately measure volumes of very viscous crude oils. For the low temperature measurements

the oils were held in a liquid nitrogen cooled, heating-freezing stage (Linkam TMS600). The sample was mounted on a cooling block inside the chamber which was fitted with an optically transparent quartz window. The temperature was controlled by varying the flow of liquid nitrogen from a Dewar flask to the stage, and a minimum temperature of 133 K was possible with an accuracy of approximately 0.1 °C. Below ~200 K to prevent condensation forming on the stage windows a flow of dry nitrogen gas was directed onto the window during measurements. Temperature calibration was performed on a bi-monthly basis using the phase transition points (homogenization temperature) for two synthetic fluid inclusion standards (H_2O and CO_2).[33] The water inclusion standard covered the 163 to 293 K range with a homogenization temperature of 216.4 K. The CO_2 inclusion covered the 223 to 673 K range, with a homogenization temperature of 663 K. The homogenization temperatures of the fluid inclusions were determined by microscope observation.

Fluorescence Instrumentation. For lifetime analysis of the crude oil samples, two Time Correlated Single Photon Counting (TCSPC) fluorescence lifetime measurement systems using a 405 nm excitation source (Figure 1 & supplemental information) were assembled in house.

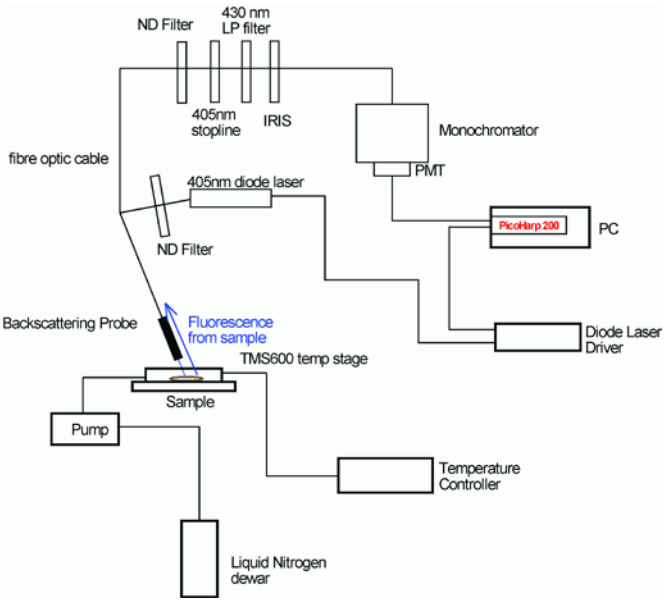

Figure 1: Schematic of the low temperature measurement system used to collect the fluorescence lifetime and steady-state data from the diluted crude oils. The excitation is provided by a 405 nm pulsed laser diode and the detection system is a TCSPC system with high timing resolution (PicoQuant GmbH, Berlin). See the supplemental information for full details of the instrumentation.

Fluorescence Measurements. The fluorescence lifetimes of the neat crude oil samples were measured at set emission wavelengths between 430 and 540 nm at 10 nm intervals between 133 K and 298 K. For low temperature experiments, a drop of neat non-degassed oil was placed onto a quartz dish and sealed within the stage chamber. A positive pressure of nitrogen was maintained to provide an oxygen free environment within the chamber during cooling (effectively degassing the oil). The temperature was decreased at a cooling rate of 20 degrees per minute, in 20 K increments, followed by a 20 minute equilibration period in the dark. The excitation light was then applied to the sample for one minute, prior to data acquisition. Since, dissolved oxygen has a large quenching effect on aromatic hydrocarbon fluorescence,[34]

deoxygenation of the dilute oils was necessary. After dilution, the samples were thoroughly mixed and then purged with oxygen-free nitrogen for 15 minutes. A slow flow rate was maintained to minimize sample evaporation and the fluorescence lifetime was measured *in-situ* every 5 minutes. After deoxygenation, the sample vials were moved to a nitrogen filled atmospheric bag (Aldrich) where the sample was transferred by syringe to a small quartz crucible (circa 4 mm deep), before covering with a quartz lid and sealing with PTFE and laboratory film. This was then transferred to the temperature stage (Nitrogen purged) and the fluorescence lifetime was recorded and compared to the value recorded during the degassing stage to ensure no oxygen had redissolved in the sample. Fluorescence lifetimes were recorded between 450 and ~600 nm (20 nm intervals) over a range of temperatures from 293 K to 93 K (20 K intervals).

Deconvolution and fitting of the fluorescence decays was performed using Fluofit software (Picoquant, Version 4.2). For all neat oil lifetime measurements, the data was collected to 10K counts in the channel of maximum intensity. Replicate experiments at 273 and 213 K determined that the lifetime measurement repeatability was ~0.1 ns with a standard deviation ranging between 0.03 and 0.06 ns. The lifetime fitting error was determined by support plane analysis.[31]

Results and Discussion

An extensive array of data was collected, and this was analyzed in the following sequence. First we examined the gross changes in the emission data (lifetime and steady-state emission) with temperature and dilution. We then explained the changes in terms of a holistic model dominated by energy transfer (ET) and quenching processes. The second stage of the analysis involved an attempt to correlate the observed changes with compositional data for these oils generated via a standard SARA analysis.[29,30] The third stage in the data analysis involved modeling the observed temperature induced changes in the fluorescence emission while the oils were still liquid and thus where collisional quenching (which is diffusion based) was likely to be the dominant factor involved. Finally we studied in detail the anomalous behavior of fluorescence emission at the lowest temperature where the oils are completely frozen and diffusion based processes should not occur.

Influence of temperature on lifetime and steady state intensity measurements. Cooling the neat crude oils caused a significant increase in fluorescence intensity (up to 20-25%) accompanied by a dramatic increase in average fluorescence lifetimes (Figure 2). The lighter, less viscous oils, which generally have lower quencher concentrations, exhibited a greater lifetime increase over this temperature range. This indicated that quenching was the dominant factor affected by lowering the temperature. The largest changes in fluorescence lifetime and intensity occurred above ~170-200 K, below which the lifetime remained constant or decreased by a small, yet very significant amount. The small lifetime decreases observed below ~170-200 K were not due to factors such as refractive index changes or increased scattering contribution, but rather to an increase in vibrational relaxation rates, *vide infra*. The heavy, viscous oils

showed only a very small increase in lifetime over the temperature range because of the relatively higher concentrations of quenching species present.

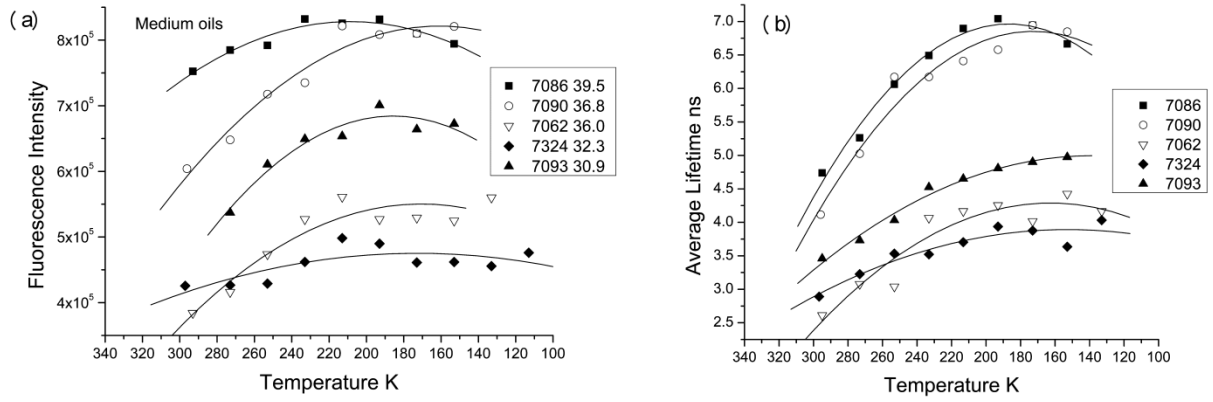

Figure 2: **(a)** Variations in Fluorescence intensity for four medium density neat crude oils. Intensity increases of up to ~25% were obtained at low temperatures. **(b)** Average lifetimes for the same set of oils over the range of recorded temperatures. This figure shows a representative sample set of 5 oils, the others were omitted for clarity.[39]

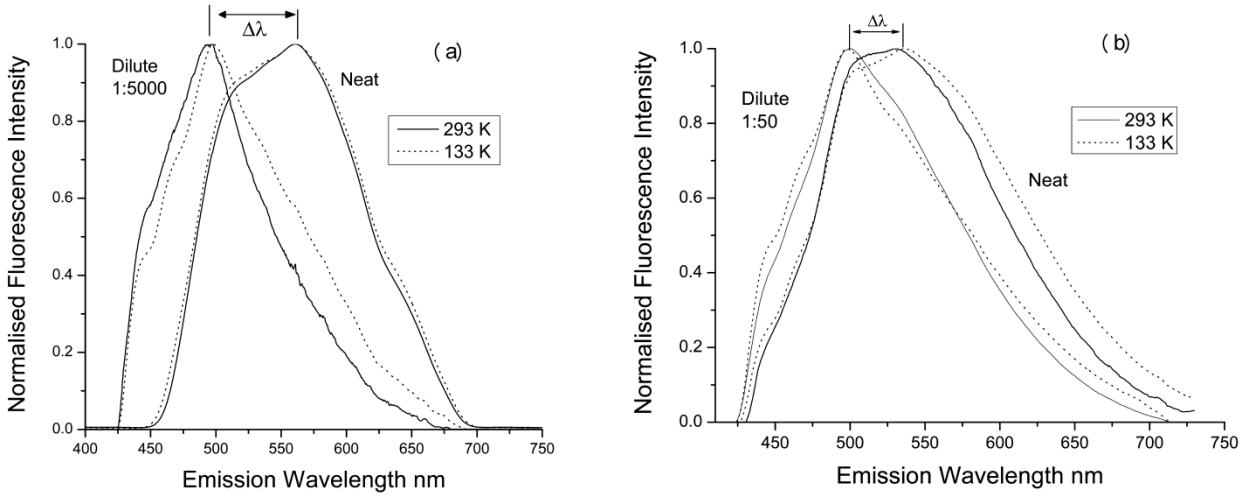

Figure 3: **(a)** Normalized emission spectra for neat and diluted (deoxygenated) heavy oil 7033 at 293 and 133 K ($\Delta\lambda_{293K}$= 67 nm, $\Delta\lambda_{133K}$= 65 nm). **(b)** Normalized emission spectra for neat and diluted light oil 7197 at 293 and 133 K ($\Delta\lambda_{293K}$= 31 nm, $\Delta\lambda_{133K}$= 38 nm). For the dilute oil (1:50 was used due to very weak spectra obtained at higher dilutions), the spectrum does not change considerably.

The normalized emission spectra for neat and dilute oils at 293 and 133 K (Figure 3), showed that while dilution caused blue shifts of different magnitudes for heavy and light oils, there was no corresponding wavelength shift with decreasing temperature although a broadening of the emission spectra could occur. Spectra from heavy oils (higher concentrations of polar and large aromatic species) showed a significant dilution-induced blue shift (Figure 3a). On lowering the temperature the spectra from the diluted heavy oils were broadened and showed a very small red shift. However there was no significant change in the emission spectra of the neat heavy oil when the temperature was lowered. This implied that for heavy oils, dilution caused very large changes in ET, whereas temperature changes influenced quenching much more than ET. For light oils (Figure 3b), the dilution induced blue shift was less than that for the heavy oils, and there was a small emission band broadening for the neat oil but not for diluted oil as the temperature was lowered. The spectral broadening for the neat light oils, was probably due to a combination of reduced collisional quenching of the red emitting, acceptor fluorophores and a reduction in the internal conversion from excited to ground state in accordance with the energy gap law.[35,36]

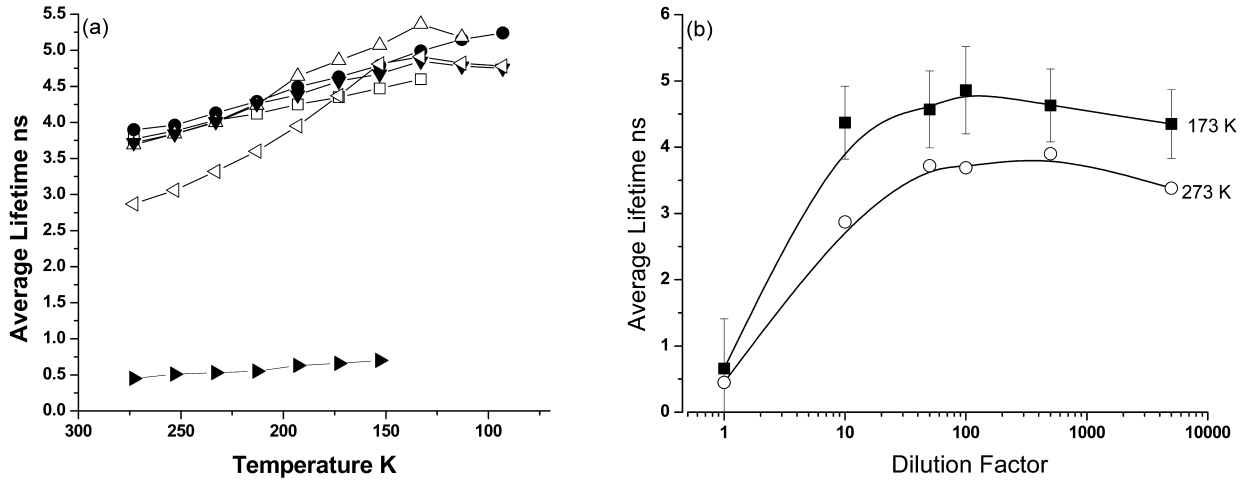

Figure 4: (a) Variation of fluorescence lifetime with temperature for a series of dilutions of oil 7033. Dilution factors are: neat (▶), 1:10 (▷), 1:50 (▼), 1:100 (△), 1:500 (●), 1:5000 (□). Generally, the lifetimes increase to a high point temperature where no further significant changes are found. (**b**) Variation of average lifetime of the oil (taken at: 173K (■) and 273K (○)) with dilution. The error bars represent one standard deviation on the average lifetime and were calculated by support-plane analysis. Emission wavelength 500 nm.

The effect of decreasing temperature on lifetime was much greater for the diluted oils than for the neat oils (Figure 4a). At higher dilutions (>1:100) the temperature-lifetime plots were very similar for the higher (>200 K) temperatures, but there are some significant variations below 200 K. This variation may be due to changes in vibrational relaxation. An alternate way of presenting this data (Figure 4b) shows two plots of lifetime versus dilution at 273 and 173 K. The lifetime increased with dilution up to a maximum ($\tau_{\lambda max}$), depending on the type of oil, which for oil 7033, was a dilution factor of 1:100. At higher dilutions where collisional quenching and ET are minimized, the slight reduction in lifetime observed may be attributed to

an increased scattering contribution as sample absorbance decreased, but, we also note this was within the measurement error.

Correlation of lifetime-temperature data with chemical composition. The next stage in the data analysis involved trying to correlate the low temperature fluorescence lifetime data with the gross chemical compositional data generated via chromatographic methods.[29] Previous studies using 405 nm excitation at ambient temperatures showed that there were no good and accurate correlations between fluorescence lifetimes and API gravity, polar, asphaltene, aromatic or alkane fractions.[30, 31] This was ascribed to the sheer complexity of the neat crude oils, and it was postulated that cooling of the oils in order to minimize quenching may improve the correlations between the spectral and compositional data. Unfortunately this was not the case and we could not generate any other models that were an improvement on the correlations obtained at ambient temperatures.[39] Figure 5 shows typical examples of the correlations obtained at ambient and low temperature. In all cases the degree of scatter was very substantial and not reduced by cooling. However, the interesting behavior of the fluorescence emission at low temperatures for these very complex oils warranted further investigation.

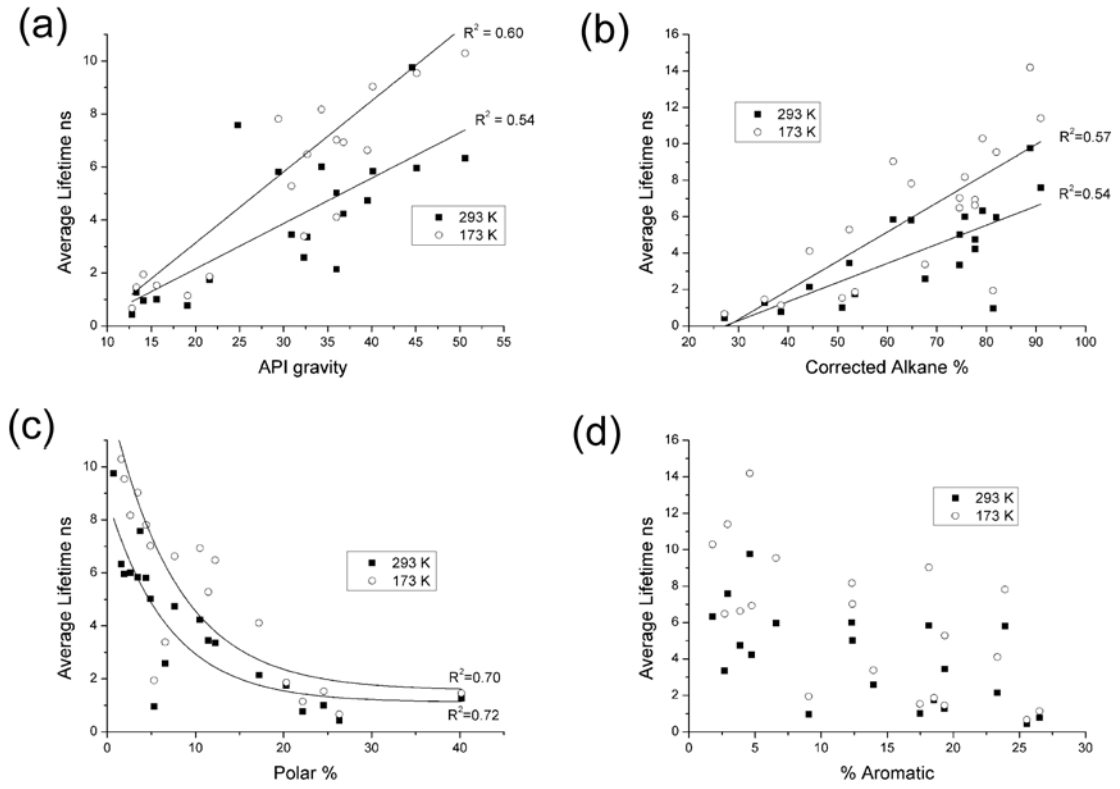

Figure 5: Scatter plots showing correlations between average fluorescence lifetimes (measured at 500 nm) and (a) API gravity, (b) corrected alkane concentration, (c) polar concentration, and (d) aromatic concentration. The compositional data was published in references 29 and 30.

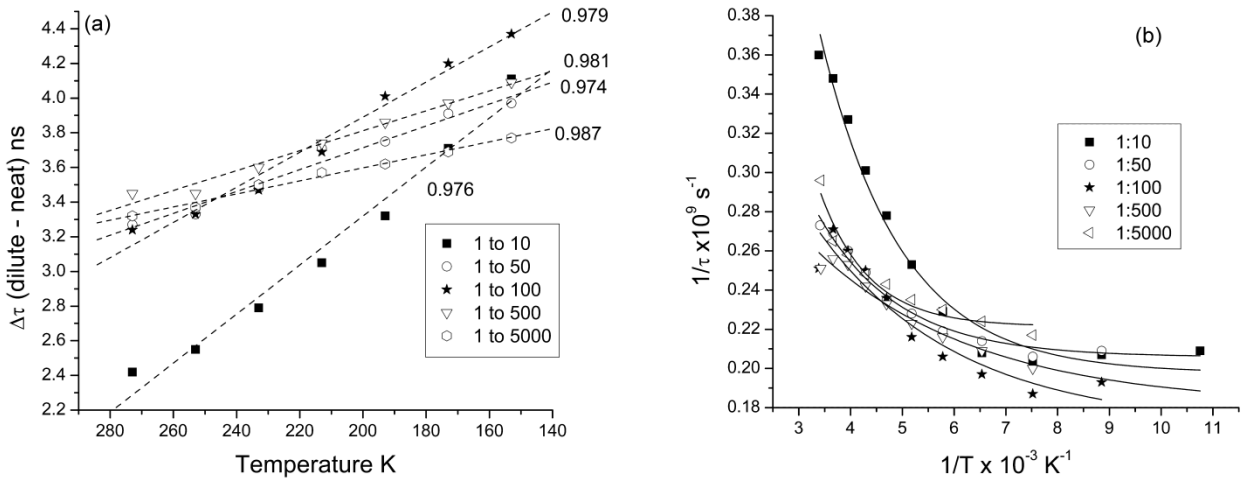

Figure 6: (a) Plot of the difference between neat and dilute lifetimes for oil 7033 over the 150 to 280 K range. The lifetime difference increases gradually as the temperature decreases but at varying rates as shown by the slope of each plot. Correlation coefficients (r^2) are given for each linear fit. **(b)** Arrhenius plot for a heavy oil 7033 diluted from 1:50 to 1:5000 in 3:2 MeCH:MeCP. All data measured at an emission wavelength of 500 nm.

Arrhenius temperature dependence of crude oil lifetimes. We observed that the difference between the average lifetimes of the neat and diluted oils ($\Delta\tau$) decreased linearly as the temperature dropped (Figure 6a) and the biggest rate of change occurred at a 1:10 dilution. The linear behavior of the T-$\Delta\tau$ plots indicated that the processes governing fluorescence emission varied in a systematic fashion and that it may be possible to quantitatively model these effects. The fact that the largest change was observed at 1:10 was to be expected because at this dilution, quencher concentration was still relatively high and thus the rate of collisional quenching was

still significant. This is in contrast with the very high dilution case (1:5000) where collisional quenching was expected to be much lower.

The temperature dependant lifetime data for dilute (Figure 6b) and neat oils (Figure 7a) were modeled using the Arrhenius equation:

$$\frac{1}{\tau_T} = \frac{1}{\tau_0} + A\exp\left(\frac{-E_{NR}}{RT}\right) \quad \textbf{(1)}$$

where E_{NR} is an activation energy for the diffusional based processes that compete with fluorescence ($kJmol^{-1}$), R is the gas constant and A is the pre-exponential factor (s^{-1}) of the temperature-dependent process.[14,37] Since we can not explicitly measure fluorophore concentration in crude petroleum oils, we argue that this activation energy relates to a mole *of emitting fluorophores*. The Arrhenius model implied that for crude oil fluorescence emission, the conversion to the ground state was composed of a temperature-dependent component (diffusion based collisional quenching) and a temperature-independent part (static quenching and ET).[37] Non-linear least squares fitting of the data yields values for A, E_{NR} and τ_0 for neat crude oils (Table 1) and some diluted oils (Table 2). The intrinsic lifetime, τ_0, was a robust measure of the static quenching present in the cold, yet still liquid state because it increased significantly with API gravity (S-5a), decreased with increasing polar content (S-5b), , and increased significantly with the degree of dilution. The accuracy of the E_{NR} and A values are less certain as there were too few data points (6 to 9) to generate consistent values for the complete range of oils. However, the E_{NR} range of 4.6-27.2 $kJmol^{-1}$ (av. = 13.6, SD = 6.4 $kJmol^{-1}$) was typical of the activation energies involved in the quenching of fluorophores in solution.[38] These values were also very similar to the activation energies for thermal quenching measured in high

temperature studies of crude oils.[9] We found no clear good correlations between E_{NR} or A values with any of the oil compositional data (not shown).[39]

Table 1 here.

Table 2 here.

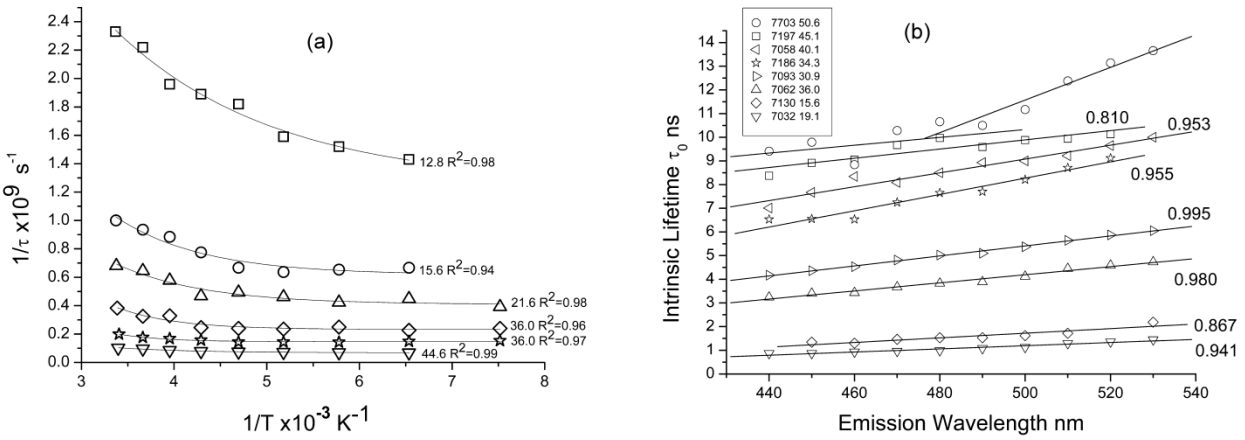

Figure 7: (a) Effect of temperature on average lifetimes for 6 representative crude oils. Also shown is the non-linear least squares fitting line for the Arrhenius model: (7033 (□), 7130 (○), 7169 (△), 7062 (◇), 7193 (☆), oil 7098 (▽), All data measured at an emission wavelength of 500 nm.; **(b)** Variation of intrinsic lifetime with emission wavelength for a series of neat crude oils covering a wide API gravity range (19.1-50.6).

Table 3 here.

Another interesting facet of the Arrhenius modeling was the emission wavelength effect (Figure 7b and Table 3), where τ_0 varied linearly in the 440-540 nm range whereas A and E_{NR} values did not change with any discernable pattern. The smaller τ_0 change for heavy and medium oils arose from the relatively high quencher concentrations present, which masked other competing photophysical processes. The increase in lifetime from blue to red emission wavelengths originated from ET, and was related to the increasing contribution from the red acceptor fluorophore emission.[40] The lightest oil, #7703, showed very different behavior with two distinct linear regions which probably occurred because of its very low polar (1.58 %) and aromatic content (1.79 %).[30] This ensured a very low level of static fluorescence quenching, which enabled the observation of subtle ET effects and thus we observed decreased donor lifetimes (blue) and larger increased acceptor lifetimes (red). The next lightest oil #7197, however, showed a linear wavelength dependence as a result of its significantly higher polar (1.97 %) and aromatic concentrations (6.59 %) which caused a much larger degree of static quenching. This was compatible with the observed changes in the emission bandwidth on cooling for the light and diluted heavy oils (Figure 3). For these samples we saw more red emission from the acceptors, as a result of the reduced collisional quenching of the red emitting fluorophores.

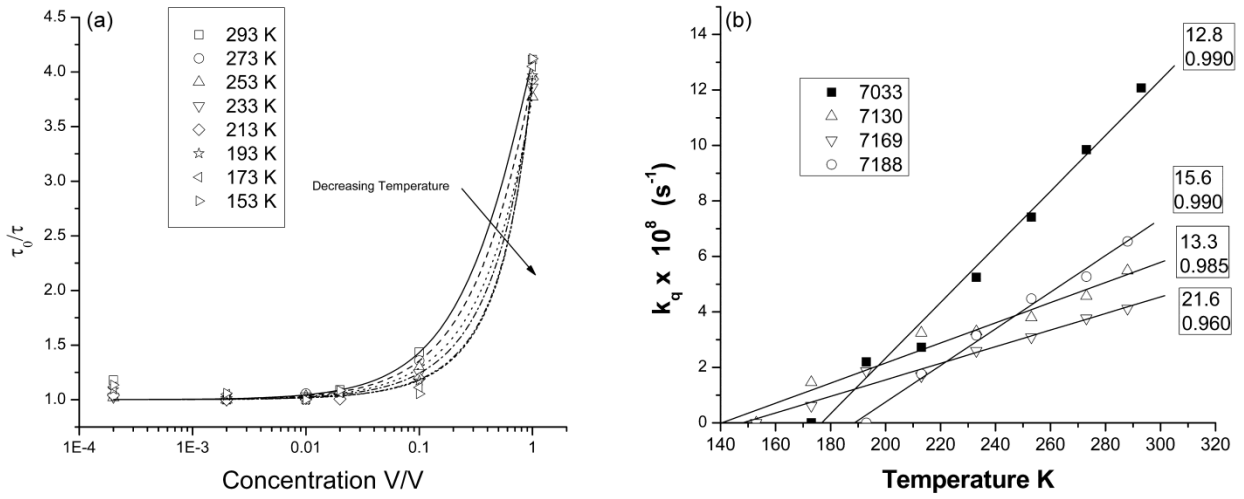

Figure 8: (a) Modified Stern-Volmer plots for heavy oil 7033 over a range of temperatures. De-oxygenated solutions were used throughout. **(b)** Pseudo collisional quenching constant as a function of temperature for several oils. API gravity values and correlation coefficients (r^2) are also given. All data measured at an emission wavelength of 500 nm.

Assessment of quenching mechanisms. It was clear that we needed to assess the relative contributions from the static and collisional fluorescence quenching mechanisms. This was achieved using a modified Stern-Volmer (mS-V) equation (supplemental information). For example, mS-V plots were prepared from lifetimes recorded for the diluted 7033 oil at different temperatures (Figure 7a and Table S-1 supplementary information) where τ_0 was the maximum lifetime estimated from the Arrhenius fits to the diluted oils (Table 2). As the temperature dropped to 193 K, viscosity increased, which slowed the collisional quenching rate, and this in turn led to a progressive decrease in the pseudo bimolecular quenching constant (pK_{SV}) values from a maximum of ~12×10^8 s^{-1} to ~2.2×10^8 s^{-1} (Table S-1 supplementary information). We used the term pseudo here, because fluorescence emission originated from a wide variety of different fluorophores, and pK_{SV} represents an average value from all the individual

contributions. Once the temperature dropped below ~173 K, pK_{sv} tended to zero and K_{st} increased dramatically because all diffusional motion ceased and the only quenching observed was the static component. The k_q values obtained here, are of similar magnitude to those reported for the fluorescence quenching of naphthalene by organic dienes in cyclohexane,[41] and amines in water.[42] While this comparison was not entirely valid because of the massive differences in composition/complexity it did indicate that the fluorescence quenching behavior was very similar. It was also probable that some of the observed quenching originated from exciplex formation in these complex fluids; however, we were unable to obtain any unambiguous evidence from the emission data to validate this claim.

The linear variation of the pseudo k_q values with temperature for four different heavy oils (Figure 8b) showed that the relationship between dynamic quenching and temperature was very composition dependent. Oils 7033 and 7188 had the steepest slopes because the viscosity of these oils decreased the quickest as the temperature dropped. This was not surprising for these particular oils because they both have a relatively high combined wax and asphaltene concentration (7033: 17.9%, 7188: 18.9%) compared to the other two oils (7130: 2.15%, 7169: 5.7%). For the 7062 oil (14.86%), the slope was intermediate between the two groups (data not shown). It is well known that both Asphaltenes and waxes have a very large influence on the viscosity/mobility of crude oils; we expect that oils with high concentrations of these constituents would become immobile at higher temperatures.[43]

Eyring temperature dependence of crude oil lifetime data – the role of static quenching. When the oils were frozen into a solid state, we often observed a small drop in lifetime as the temperature dropped below ~200 K which obviously cannot be due to collisional quenching.

This was unexpected and we think that it was due to an increased vibrational coupling rate (k_{VC}) between the fluorophores and the surrounding matrix. We base this on the assumption that the ET rate was not affected by the temperature drop in the 100-200 K region. We modeled this behavior by considering that a "dark, non-fluorescent intermediate" was formed by vibrational coupling between the excited fluorophore and the surrounding matrix. This is analogous to the activated complex in Transition State (TS) theory.[44] We found that the fluorescence lifetime changes for both neat and dilute oils at low temperature fitted very well (Figure 9) to the Eyring equation:

$$\ln\left(\frac{k_{meas}}{T}\right) = -\frac{\Delta H^{\ddagger}}{RT} + \frac{\Delta S^{\ddagger}}{R} + \ln\left(\frac{k_B}{h}\right) \qquad \textbf{(2)}$$

The fluorescence rate constant (k_{meas}) at any given temperature was inversely related to the concentration of the dark/quenched complex. k_{meas} was obtained from the reciprocal of the measured fluorescence lifetime ($1/\tau$), R is the gas constant ($JK^{-1}mol^{-1}$), k_B is Boltzmann's constant, and h is Planck's constant. Thus $\triangle H^{\ddagger}$ represented the enthalpy associated with the vibrational coupling process and $\triangle S^{\ddagger}$, the associated entropy, is a measure of the probability of quenching. The decrease in the fluorescence lifetime at low temperature (<200 K) thus represented an increased dark species concentration caused by an increase in vibrational coupling efficiency in the lattice. The slopes ($\triangle H^{\ddagger}/R$) of the plots for all oils were very similar which indicates that the process was essentially the same for all oils, The recovered values for $\triangle H^{\ddagger}$ (Table 4) were all relatively small at ~ -1.2 $\pm$ 0.5 $kJmol^{-1}$, which is typical for low energy lattice vibrations. The negative value was a consequence of the fact that we modeled/measured the dissociation of the dark complex via the fluorescence emission. On changing from the heavy to the light oils, the Gibbs free energy at 153 K increased as expected, and spanned a range of +9.8

to +13.7 kJmol^{-1}, which reflected the decreasing spontaneity of the vibrational coupling process as the oils became less complex.

Table 4 here.

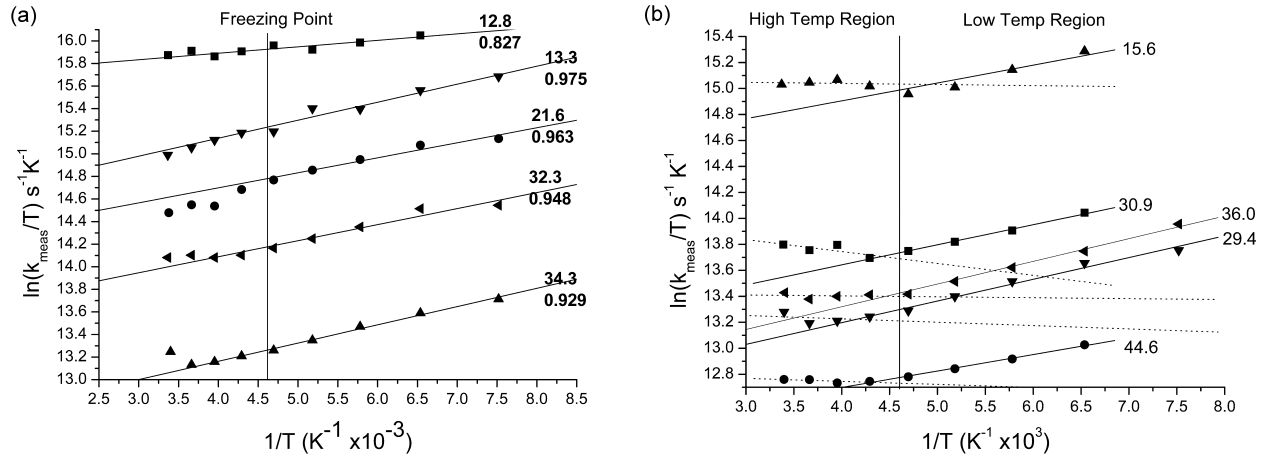

Figure 9: Eyring plots and associated linear fits for: **(a)** Heavy oils ■: 7033,▼:7188, ●: 7169, ◀: 7324, ▲: 7186. API gravity and correlation coefficients (r^2) are also shown for each plot. **(b)** Light-medium oils: ▲:7130, ■:7093, ◀:7193, ▼:7187, ●:7098. The vertical line separates the higher and lower temperature domains at ~213 K. All data measured at an emission wavelength of 500 nm.

The extent of the linear region varied according to the oil, and for some heavy oils (e.g. 7033/7188, Figure 9a) we get linear behavior up to room temperature. This linear behavior occurred because static quenching via vibrational coupling was dominant in these oils. In general, for the neat crude oils, the Eyring-based relationship broke down as the temperature increased above ~213 K where the oils become liquid and collisional quenching starts to

dominate. The freezing point of the oils varied according to API gravity, Asphaltene and wax concentration. For some oils, we clearly observed a two phase behavior, where the slope of the plot in the liquid phase was opposite in sign to that of the low temperature, solid state. The heavy oil #7130 (▲ Figure 9b) appeared to be peculiar, but when compared to the other heavy oils (7033/7188) with similar API gravity, one noted that it had a much higher alkane concentration and much lower asphaltene/wax concentration, and thus likely to be less viscous and freeze/solidify at a lower temperature.

The magnitude of $\triangle S^{\ddagger}$ gave a measure of the sensitivity to static quenching. This was so because vibrational coupling based quenching involved a fluorophore and an appropriate matrix molecule coming together and forming a transient (very briefly) complex (or better a very loose association), thus generating a more ordered state. The likelihood that there was a quencher molecule with appropriate vibrational energy levels in close proximity increased for the heavier oils, thus $\triangle S^{\ddagger}$ decreased. There was a non-linear exponential correlation between $\triangle S^{\ddagger}$ and τ_0 calculated using the Arrhenius equation with a best fit equation of $\tau_0 = ae^{b\triangle S^{\ddagger}}$ (r^2 = 0.914, supplemental information S-6). This showed clearly that there was a connection between the Arrhenius and Eyring models for fluorescence quenching in crude oils. We also noted that as the emission wavelength increased, $\triangle S^{\ddagger}$ increased in accordance with the energy gap law (supplemental information Table S-2), because the rate of the competing internal conversion route increased with decreasing emitted photon energies.

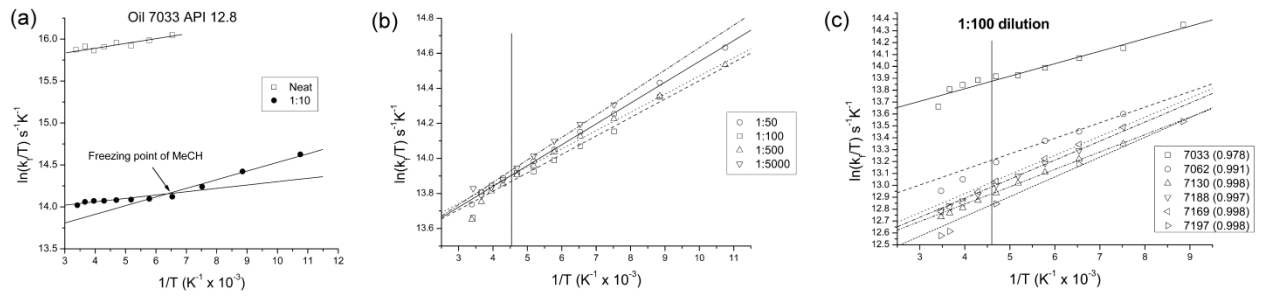

Figure 10: Eyring plots and associated linear fits for: **(a)** Heavy oil 7033 neat and at a dilution of 1:10, **(b)** Heavy oil 7033 at dilutions of between 1:50 and 1:5000. **(c)** A selection of oils at a dilution of 1:100, shown linear correlation coefficients shown in brackets. The linear fit region was set to the 133-213 K temperature range for all oils. All data measured at an emission wavelength of 500 nm.

The diluted crude petroleum oils (Table 5) followed similar trends, with $\triangle H^{\ddagger}$ remaining constant and a significant change in $\Delta S^{\ddagger}$ on dilution. This was as expected because dilution caused a separation of fluorophore and quencher molecules, reducing the probability of vibrational coupling. The change was relatively large for the heavy oils (20-30%) but was much smaller (~3%) for the light oils. Since the both the neat and diluted oils all showed very similar behavior below ~200 K, we concluded that the same vibrational relaxation mechanism operated in each case. For some oils, at the 1:10 dilution stage we obtained a bilinear plot (Figure 10a) with a transition point which corresponded to the freezing point of the MeCH:MeCP solvent mixture. The linear behavior of the neat oil corresponded to a consistently high level of static quenching. When the oil is diluted to 1:10 it caused a large change in the average fluorophore-quencher separation. This resulted in reduced static quenching in the solid phase, but in the

liquid phase, this level of dilution was not sufficient to completely eliminate collisional quenching, and thus the relationship changed giving a bilinear plot. At the higher dilutions (Figure 10b), collisional quenching was minimized, and consequently the Eyring plots reverted to a largely linear correlation because the primary non-radiative decay pathway was via vibrational coupling. When we compared several different diluted oils (Figure 10c and Table 5) we got very similar slopes (and $\triangle H^{\ddagger}$ values) irrespective of oil type. This was to be expected since this vibrational coupling process should be reasonably independent of oil composition at high dilutions.

Table 5 here.

Conclusions

The measurement of fluorescence emission from crude petroleum oils at low temperatures showed systematic behavior in both the time-resolved and steady state emission data. Modeling of this temperature dependant emission properties provided a better understanding of the interplay between static/dynamic quenching and energy transfer in these complex petroleum fluids. Modified Stern-Volmer analysis of the fluorescence data collected from the diluted oils showed that collisional quenching was the dominant process operating in the liquid phase for the neat to 1:50 dilution range. We observed that all the crude oils (diluted or neat) in the liquid state where collisional fluorescence quenching was dominant followed a simple Arrhenius temperature dependence. In this ambient-to-cold liquid state, the Arrhenius model enabled the calculation of an intrinsic lifetime τ_0 which was inversely related to the degree of static fluorescence quenching present. Once the oil samples (neat or dilute) become frozen, we then observed the much weaker non-radiative decay pathway via vibrational coupling (k_{VC}) to the surrounding matrix.

At very low temperatures, when frozen in a solid state, the primary non-radiative decay pathway for the fluorophores was via vibrational coupling to the surrounding matrix and this could be modeled by the Eyring equation. This non-radiative decay pathway was a low energy process (~1 kJ.mol^{-1}) which was a consequence of the fact that in these complex crude oils, there was an extensive overlap of vibrational states between fluorophores and quenching molecules in the surrounding matrix, which provides for an efficient coupling process in the frozen solid state. The vibrational coupling pathway competed with the internal conversion route (as per energy gap law) and became a relatively larger contributor to the overall non-radiative

decay rate as the temperature dropped. We observed that the magnitude of the enthalpy was largely independent of the degree of oil dilution or type whereas the entropy was dependent on oil type, and gave a measure of the degree of static quenching.

Acknowledgements

This work was supported by Science Foundation Ireland under Grant number 05/RFP/GEO0002. The authors would like to thank Dr. M. Feely of the Department of Earth and Ocean Sciences for the loan of the Linkam temperature stage. We thank Dr.'s N. Blamey, B. Szczupak, and R. Murray for their help and advice during the early stages of the work on the neat crude oil samples.

Supporting Information Available

More details of the instrumentation, measurement methods, and additional spectral information is provided in the supporting information. This information is available free of charge via the Internet at http://pubs.acs.org/ .

References

(1) Bourgougnon, A. *J. Am. Chem. Soc.* **1879**, *1*, 188-204.

(2) Ryder, A. G. *Reviews in Fluorescence Annual Volumes* **2005**, 169-198.

(3) Ralston, C.; Wu, X.; Mullins, O. *Appl. Spectrosc.* **1996**, *50* (12), 1563-1568.

(4) Downare, T. D.; Mullins, O. C. *Appl. Spectrosc.* **1995**, *49* (6), 754-764.

(5) Wang, X.; Mullins, O. C. *Appl. Spectrosc.* **1994**, *48* (8), 977-984.

(6) Smith, G. C.; Sinski, J. F. *Appl. Spectrosc.* **1999**, *53* (11), 1459-1469.

(7) Patra, D.; Mishra, A. K. *Polycycl. Aromat. Compd.* **2001**, *18* (4), 381-396.

(8) Patra, D.; Mishra, A. K. *Talanta* **2001**, *53* (4), 783-790.

(9) Zhu, Y.; Mullins, O. C. *Energy & Fuels* **1992**, *6* (12), 545-552.

(10) Huang, W. L.; Otten, G. A. *Org. Geochem.* **2001**, *32* (6), 817-830.

(11) Stout, S. A.; Lin, R. In *7th Annual Meeting of the Soc for Organic Petrology*; Pergamon-Elsevier Science Ltd: Calgary, Canada, 1990, p 229-239.

(12) Huang, W. L.; Otten, G. A. *18th International Meeting on Organic Geochemistry* **1997**, 1119-1137.

(13) Chang, Y. J.; Huang, W. L. *Geochim. Cosmochim. Acta* **2008**, *72* (15), 3771-3787.

(14) Bowen, E. *Faraday Discuss.* **1959**, *27*, 40-42.

(15) Futoma, D. F.; Smith, S. R.; Tanaka, J. *Crit. Rev. Anal. Chem.* **1982**, *13* (2), 117-154.

(16) Gooijer, C.; Kozin, I.; Velthorst, N. H. *Mikrochim. Acta.* **1997**, *127* (3-4), 149-182.

(17) Garrigues, P.; Ewald, M. *Int. J. Environ. Anal. Chem.* **1985**, *21* (3), 185-197.

(18) Garrigues, P.; Bellocq, J.; Wise, S. A. *Fresen. J. Anal. Chem.* **1990**, *336* (2), 106-110.

(19) Zhang, W.; Lin, D.; Zou, Z.; Li, Y. *Talanta* **2007**, *71* (4), 1481-1486.

(20) Dickinson, R. B.; Wehry, E. L. *Anal. Chem.* **1979**, *51* (6), 778-780.

(21) Bark, K. M.; Force, R. K. *Appl. Spectrosc.* **1990**, *44* (8), 1373-1376.

(22) Bystol, A. J.; Yu, S.; Campiglia, A. D. *Talanta* **2003**, *60* (2-3), 449-458.

(23) Fortier, S. H.; Eastwood, D. *Anal. Chem.* **1978**, *50* (2), 334-338.

(24) Lloyd, J. B. F. *Analyst* **1980**, *105* (1247), 97-109.

(25) Chukova, O.; Krut, O.; Nedilko, S.; Sakun, V.; Scherbatskyi, V. *Ann. Chim-Rome* **2005**, *95* (11-12), 885-895.

(26) Corfield, M. M.; Hawkins, H. L.; John, P.; Soutar, I. *Ananlyst* **1981**, *106* (1259), 188-197.

(27) Ryder, A. G. *Appl. Spectrosc.* **2002**, *56* (1), 107-116.

(28) Ryder, A. G.; Glynn, T. J.; Feely, M.; Barwise, A. J. G. *Spectrochim. Acta A,* **2002**, *58* (5), 1025-1037.

(29) Ryder, A. G. *Appl. Spectrosc.* **2004**, *58* (5), 613-623.

(30) Ryder, A. G.; Przyjalgowski, M. A.; Feely, M.; Szczupak, B.; Glynn, T. J. *Appl. Spectrosc.* **2004**, *58* (9), 1106-1115.

(31) Owens, P.; Ryder, A. G.; Blamey, N. J. F. *J. Fluoresc.* **2008**, *18* (5), 997-1006.

(32) Montalti, M. *Handbook of Photochemistry*; CRC Press LLC: Boca Raton, USA, 2006.

(33) Macdonald, A. J.; Spooner, E. T. C. *Econ. Geol.* **1981**, *76* (5), 1248-1258.

(34) Canuel, C.; Badre, S.; Groenzin, H.; Berheide, M.; Mullins, O. C. *Appl. Spectrosc.* **2003**, *57* (5), 538-544.

(35) Englman, R.; Jortner, J. *Mol. Phys.* **1970**, *18* (2), 145-164.

(36) Claude, J. P.; Meyer, T. J. *J. Phys. Chem.* **1995**, *99* (1), 51-54.

(37) Barigelletti, F.; Dellonte, S.; Orlandi, G.; Bartocci, G.; Masetti, F.; Mazzucato, U.; *J. Chem. Soc. Faraday Trans.* **1984**, *80*, 1123-1129.

(38) Turro, N. J.; Ramamurthy, V.; Scaiano, J. C. *Principles of Molecular Photochemistry: An Introduction*; University Science Books, 2009.

(39) Owens, P., PhD thesis, National University of Ireland Galway, 2010.

(40) Ryder, A. G.; *J. Fluoresc*. **2004**, *14* (1), 99-104.

(41) Murov, S. L.; Yu, L.; Giering, L. P. *J. Am. Chem. Soc.* **1973**, *95* (13), 4329-4333.

(42) Kano, K.; Takenoshita, I.; Ogawa, T. *J. Phys. Chem.* **1982**, *86* (10), 1833-1838.

(43) Schneider, M.; Andrews, A.; Mitra-Kirtley, S.; Mullins, O. *Energy & Fuels* **2007**, *21* (5), 2875-2882.

(44) Atkins, P. W.; Paula, J. D. *Physical Chemistry*; 8th ed.; Oxford University Press: Oxford, UK, 2002.

Oil	API	τ_0 (ns)	A ($x10^{10}$ s^{-1})	E_{NR} ($kJmol^{-1}$)	Oil	API	τ_0 (ns)	A ($x10^{10}$ s^{-1})	E_{NR} ($kJmol^{-1}$)
7033	12.8	0.8	0.77	4.80	7632	32.7	6.59	171.3	22.91
7188	13.3	1.43	0.06	4.60	7186	34.3	8.28	1.85	15.82
7321	14.1	2.56	0.80	5.92	7062	36	4.12	22.9	16.91
7130	15.6	1.62	1.54	8.95	7193	36	6.87	6.2	17.21
7032	19.1	1.13	3.50	10.87	7090	36.8	6.76	22.0	19.24
7169	21.6	1.87	0.04	5.79	7086	39.5	6.96	1.29	12.92
7633*	24.8	11.56	4.46	17.03	7058	40.1	9.22	1.94	14.06
7187*	29.4	7.88	16.5	20.53	7098*	44.6	14.59	1.41	13.32
7093	30.9	5.37	1.31	12.16	7197	45.1	9.9	0.55	10.81
7324	32.3	3.44	1.46	12.31	7703	50.6	11.17	0.47	10.37
7058	40.1	9.22	1.94	14.06					

Table 1: Arrhenius parameters for neat (non-deoxygenated) crude oils as determined by non-linear least squares fitting. All data measured at an emission wavelength of 500 nm. Outliers are represented by *.

Oil	API	Dilution	Arrhenius parameters			r^2
			τ_0 (ns)	A ($x10^{10}$ s^{-1})	E_{NR} ($kJmol^{-1}$)	
7033	12.8	Neat	0.8	0.77	4.8	0.982
		1:10	5.1	0.15	5.4	0.984
		1:50	4.9	0.07	5.4	0.981
		1:100	5.5	0.09	5.1	0.983
		1:500	5.4	0.03	3.1	0.996
		1:1000	4.5	0.26	8.8	0.958
7188	13.3	Neat	1.43	0.06	4.6	0.961
		1:10	10.6	0.14	7.0	0.997
		1:50	11.0	0.24	12.1	0.986
		1:100	11.1	0.51	8.8	0.987
		1:500	11.2	0.78	10.2	0.938
		1:1000	10.9	0.11	6.0	0.859
7130	15.6	Neat	1.62	1.54	8.9	0.938
		1:10	13.8	0.04	3.9	0.983
		1:50	11.2	0.53	14.0	0.970
		1:100	12.0	0.03	7.1	0.998
		1:500	11.3	0.03	7.5	0.967
		1:1000	*n/m*	*n/m*	*n/m*	*n/m*
7169	21.6	Neat	1.87	0.04	5.8	0.980
		1:10	9.1	0.04	6.2	0.996
		1:50	10.4	0.04	9.0	0.973
		1:100	10.5	0.05	10.4	0.970
		1:500	10.5	0.05	12.3	0.870
		1:1000	10.1	0.01	6.5	0.931
7062	36	Neat	4.1	22.9	16.9	0.964
		1:10	9.0	0.23	9.9	0.983
		1:50	9.4	0.03	7.1	0.987
		1:100	9.3	0.01	5.0	0.944
		1:500	*n/m*	*n/m*	*n/m*	*n/m*
		1:1000	*n/m*	*n/m*	*n/m*	*n/m*
7197	45.1	Neat	9.9	0.55	10.8	0.997
		1:10	13.0	0.74	9.9	0.968
		1:50	*n/m*	*n/m*	*n/m*	*n/m*
		1:100	*n/m*	*n/m*	*n/m*	*n/m*
		1:500	*n/m*	*n/m*	*n/m*	*n/m*
		1:1000	*n/m*	*n/m*	*n/m*	*n/m*

Table 2: Recovered Arrhenius parameters for dilute crude oils as determined by non-linear least squares fitting. In some cases it was not possible to collect good quality lifetime data at higher dilution because of weak fluorescence making the calculation of Arrhenius parameters impossible. This was the case for oils 7130, 7062 and 7197 and the missing data is represented by n/m (not measureable).

Wavelength (nm)	τ_0 **(ns)**	**A x 10^{10} (s^{-1})**	**E_{act} ($kJmol^{-1}$)**	**r^2**
440	3.24	23.9(23)	15.24(2.4)	0.975
450	3.40	16.6(15)	14.59(2.2)	0.977
460	3.43	27.7(27)	16.09(2.4)	0.977
470	3.67	23.0(23)	16.03(2.5)	0.976
480	3.83	25.6(32)	16.75(3.1)	0.966
490	3.89	30.3(44)	17.41(3.6)	0.958
500	4.12	22.9(30)	16.91(3.2)	0.964
510	4.45	10.6(16)	15.16(3.7)	0.943
520	4.59	18.5(23)	16.75(3.1)	0.966
530	4.73	34.0(47)	18.23(3.4)	0.976

Table 3: Variation of Arrhenius parameters over the emission wavelength range for a specimen oil 7062 (API gravity 40.1). Correlation coefficients are given as a measure of the goodness of

fit of the data to linear fitting. The error on the intrinsic lifetime averaged ±0.2 ns, while the error on the activation energies and pre-exponential factors is given in brackets.

Oil	$\triangle H^{\ddagger}$ kJmol^{-1}	$\triangle S^{\ddagger}$ JK^{-1}mol^{-1}	$\triangle G^{\ddagger}_{153K}$ kJmol^{-1}	Oil	$\triangle H^{\ddagger}$ kJmol^{-1}	$\triangle S^{\ddagger}$ JK^{-1}mol^{-1}	$\triangle G^{\ddagger}_{153K}$ kJmol^{-1}
7033	-0.5	-67.3	9.8	7632	-1.4	-92.0	12.7
7188	-1.3	-77.0	10.5	7186	-1.3	-93.5	13.0
7321	-0.7	-77.8	11.2	7062	-1.6	-89.1	12.0
7130	-1.5	-80.6	10.8	7193	-1.6	-93.4	12.7
7032	-1.6	-77.8	10.3	7090	-1.2	-90.7	12.7
7169	-1.1	-79.7	11.1	7086	-1.7	-93.5	12.6
7633	-1.5	-96.9	13.3	7058	-1.3	-93.8	13.1
7187	-1.4	-93.4	12.9	7098	-1.1	-96.5	13.7
7093	-1.3	-89.5	12.4	7197	-1.2	-93.6	13.1
7324	-1.2	-85.1	11.8	7703	-1.0	-93.3	13.3

Table 4: Thermodynamic parameters (errors $\Delta\mathbf{H}^{\ddagger}$ (~10-20%), $\Delta\mathbf{S}^{\ddagger}$ (~10%)) for neat crude oils recovered from fitting lifetime data to the Eyring equation. Fitting was performed using data at temperatures below 213 K. For lighter oils, the data was calculated from the linear part of the Eyring plot (i.e. the lowest temperature region).

Oil	API	Dilution	$\triangle H^{\ddagger}$ (kJmol^{-1})	$\triangle S^{\ddagger}$ (JK^{-1}mol^{-1})
7033	12.8	Neat	-0.5	-67.3
		1:10	-0.9	-85.3
		1:50	-1.0	-86.5
		1:100	-0.9	-86.2
		1:500	-0.9	-85.9
		1:5000	-1.1	-86.6
7188	13.3	Neat	-1.3	-77.0
		1:10	-0.8	-91.5
		1:50	-1.4	-95.9
		1:100	-1.3	-95.7
		1:500	-1.5	-96.8
		1:5000	-1.5	-96.7
7130	15.6	Neat	-1.5	-80.6
		1:10	-0.6	-89.5
		1:50	-1.2	-95.1
		1:100	-1.2	-95.6
		1:500	-1.3	-96.0
		1:5000	-1.4	-96.1
7169	21.6	Neat	-1.1	-81.7
		1:10	-1.1	-92.5
		1:50	-1.3	-95.2
		1:100	-1.3	-95.4
		1:500	-1.5	-96.4
		1:5000	-1.1	-93.5
7062	36.0	Neat	-1.6	-89.1
		1:10	-1.0	-92.1
		1:50	-0.8	-90.9
		1:100	-1.1	-92.7
7197	45.1	Neat	-1.2	-93.6
		1:10	-1.2	-96.0
		1:50	-1.1	-95.5
		1:100	-1.4	-97.2

Table 5: Thermodynamic parameters (errors $\Delta \mathbf{H}^{\ddagger}$ (~10-20%), $\Delta \mathbf{S}^{\ddagger}$ (~10%)) for some diluted crude oils recovered from fitting lifetime data to the Eyring equation. Fitting was performed

using data at temperatures below 213 K. For lighter oils, the data was calculated from the linear part of the Eyring plot (i.e. the lowest temperature region).